

**The Electron Plasma Frequency
in the Martian Ionosphere**

by

Donald A. Gurnett

January 23, 1998

Dept. of Physics and Astronomy
The University of Iowa
Iowa City, IA 52242

Document 97-60001

*A brief report prepared for the Mars Express Sounder Team.

I have surveyed the literature regarding the electron density in the Martian ionosphere and now have a better understanding of the implications for surface sounding. The only direct in situ measurements available were made during the descent of Viking 1 and 2 to the surface of Mars. The corresponding electron density profiles are shown in Figures 1 and 2 from Hanson et al. [1977]. These profiles were obtained at solar zenith angles of 43° and 45° , respectively. In both cases the peak electron density was about $n_e = 10^{15} \text{ m}^{-3}$, which using the formula, $f_p = 8980 \sqrt{n_e} \text{ Hz}$, where n_e is in cm^{-3} , gives a plasma frequency of about 2.8 MHz. All other electron density profiles were obtained by the radio occultation method. These involved a variety of spacecraft, such as Mariners 4, 6, 7, and 9, and Vikings 1 and 2. Since the ray path from the spacecraft to the Earth must pass through the ionosphere of Mars, the geometric constraint imposed by the orbits of Earth and Mars makes it impossible to obtain electron density profiles at solar zenith angles greater than about 130° . Figures 3 and 4, from Zhang et al. [1990a,b] show the peak electron density in the ionosphere as a function of solar zenith angle. Figure 3 shows all available data, and Figure 4 shows an expanded scale of the nighttime region at solar zenith angles greater than 90° . On both plots I have added the electron plasma frequency on the right-hand side of the plot. On the nightside some of the points are at zero electron density. This does not mean the electron density was actually zero, it simply means that the electron density was too low to measure using the radio occultation technique. In Figure 3, one can see that the electron density increases toward lower solar zenith angles, and that no measurements are available below about 43° . According to the ionospheric theory of Chapman, the maximum electron density is expected to vary as $(\cos \theta)^{1/2}$, where θ is the solar zenith angle. This dependence simply reflects the variation in the angle of incidence of the ionizing solar ultraviolet radiation on the atmosphere. Using this function, one can extrapolate the measured peak electron to the subsolar point. Figure 5 from Zhang et al. [1990a] shows two such extrapolations, one at the lower bound of the available measurements, and the other at the upper bound. The extrapolated electron densities at the subsolar point (solar zenith angle of 0°) are $n_e = 2.3 \times 10^{15}$ and $1.5 \times 10^{15} \text{ cm}^{-3}$, which correspond to plasma frequencies of $f_p = 4.3 \text{ MHz}$ and 3.4 MHz .

As one can see from the above plots, the peak plasma frequency in the ionosphere of Mars varies from a maximum of about 4.3 MHz at the subsolar point to about 500 to 800 kHz on the nightside. Very little is known about the fine-scale structure of the Martian ionosphere on either the dayside or the nightside. The nightside ionosphere of Venus, for which much better measurements are available, has considerable structure extending down to spatial scales of tens of km, with numerous low-density holes, sometimes with electron densities as low as $n_e = 10^2 \text{ cm}^{-3}$ ($f_p = 90 \text{ kHz}$). I would expect that similar fine-scale structure should exist on the nightside of Mars, with localized holes that have plasma frequencies well below 500 kHz.

Since the ionospheric electron density is controlled by the solar ultraviolet radiation, and since this flux varies with the solar cycle, one would expect that the ionospheric density will vary with the solar cycle. Generally, higher electron densities are expected during solar maximum, and lower densities during solar minimum. Figure 6 shows an illustration from Zhang et al. [1990a] that shows the expected solar cycle control, as well as the influence of solar wind pressure variations (ρv^2). Unfortunately, the available data were collected over a range of solar cycle conditions, so it is difficult to quantitatively evaluate the solar cycle effect. Vikings 1 and 2 arrived at Mars during solar minimum, and Mariner 9 (which accounts for a considerable amount of the data in Figures 3 and 4) was about half way between solar maximum and solar minimum. The next maximum in the 11-year solar cycle will be in the year 2000, so when Mars Express

arrives at Mars, we will be in the declining phase, approaching solar minimum, which will be in 2005 to 2006. The ionospheric electron densities should then be approaching their minimum values, which is a fortunate coincidence for low-frequency surface sounding. However, it is difficult to estimate how much of a reduction will occur relative to the data presented in this report. If I had to make a guess, I would say about 10 to 20%.

References

- Hanson, W. B., S. Sanatani, and D. R. Zuccaro, The Martian ionosphere as observed by the Viking retarding potential analyzers, *J. Geophys. Res.*, 82, 4351-4363, 1977.
- Kliore, A. J., G. Fjeldbo, B. L. Seidel, M. J. Sykes, and P. M. Woicesbyn, S band radio occultation measurements of the atmosphere and topography of Mars with Mariner 9: Extended mission coverage of polar and intermediate latitudes, *J. Geophys. Res.*, 78, 4331-4351, 1973.
- Luhmann, J. G., and L. G. Brace, Near-Mars Space, *Rev. Geophys.*, 29, 121-140, 1991.
- Whitten, R. C., and L. Colin, The ionospheres of Mars and Venus, *Rev. Geophys. and Space Phys.*, 12, 155-192, 1974.
- Zhang, M. H. G., J. G. Luhmann, A. J. Kliore, and J. Jim, A post-Pioneer Venus reassessment of the Martian dayside ionosphere as observed by radio occultation methods, *J. Geophys. Res.*, 95, 14,829-14,839, 1990a.
- Zhang, M. H. G., J. G. Luhmann, and A. J. Kliore, An observational study of the nightside ionospheres of Mars and Venus with radio occultation, *J. Geophys. Res.*, 95, 17,095-17,102, 1990b.

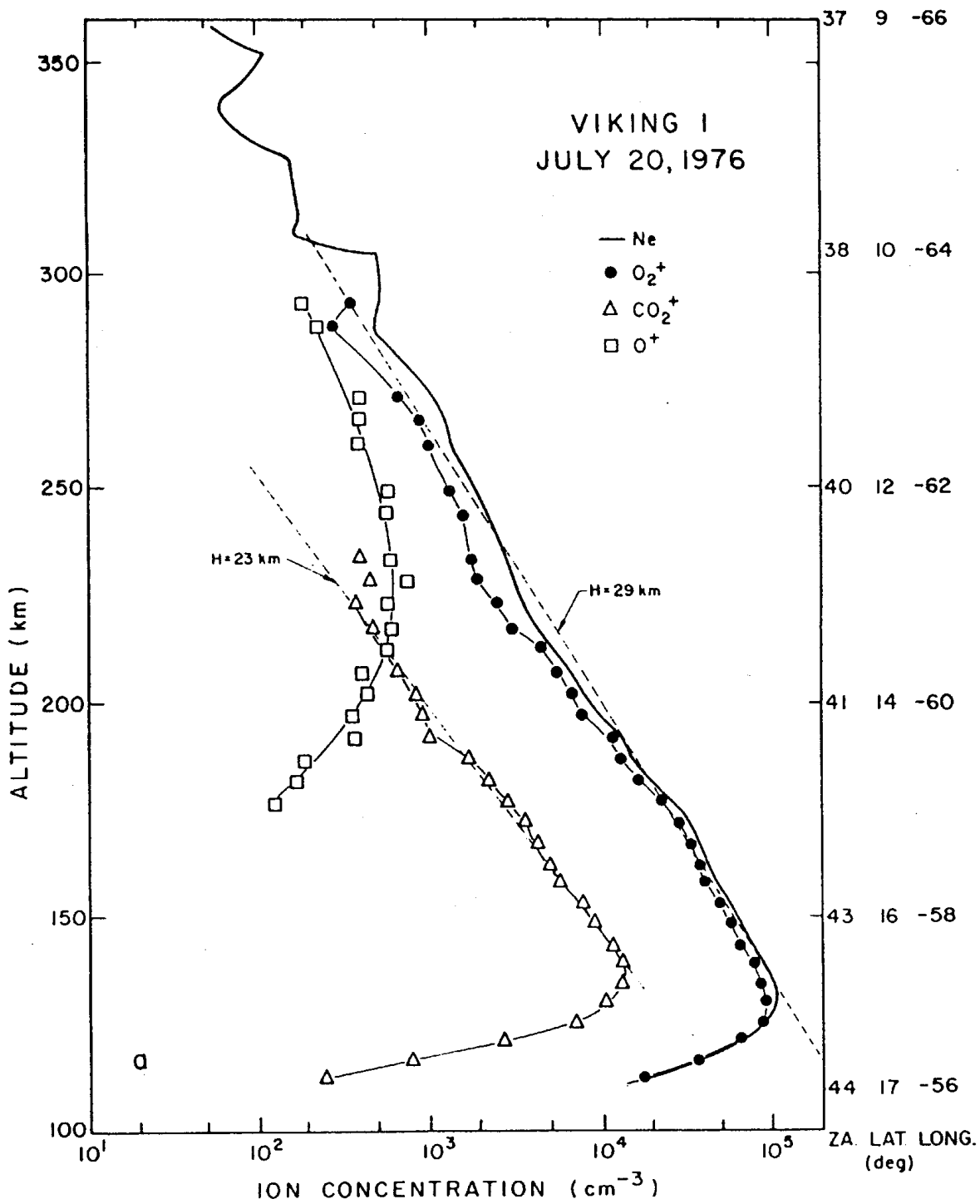


Figure 1

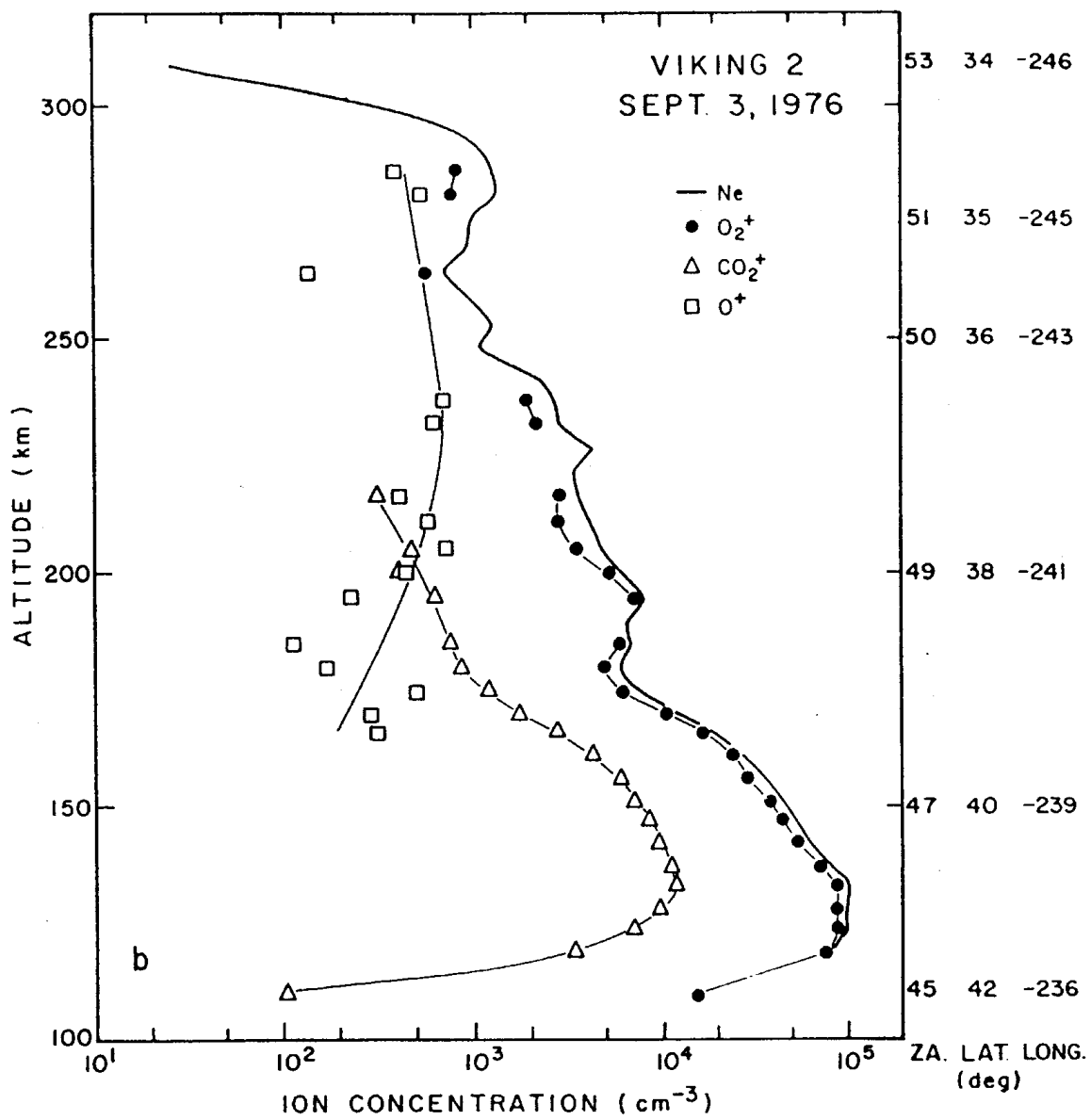


Figure 2

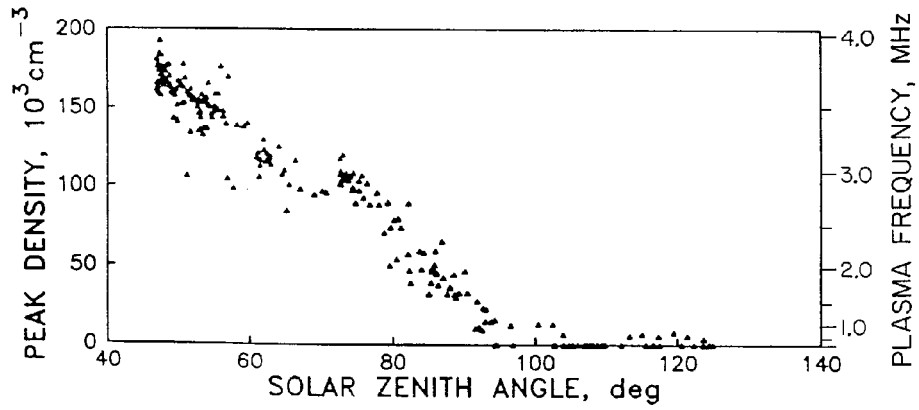


Figure 3

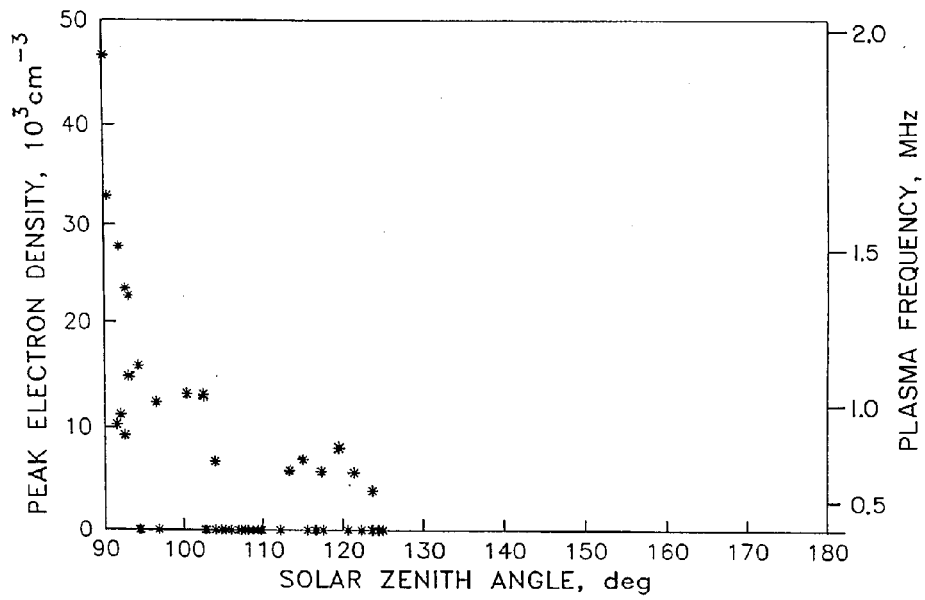


Figure 4

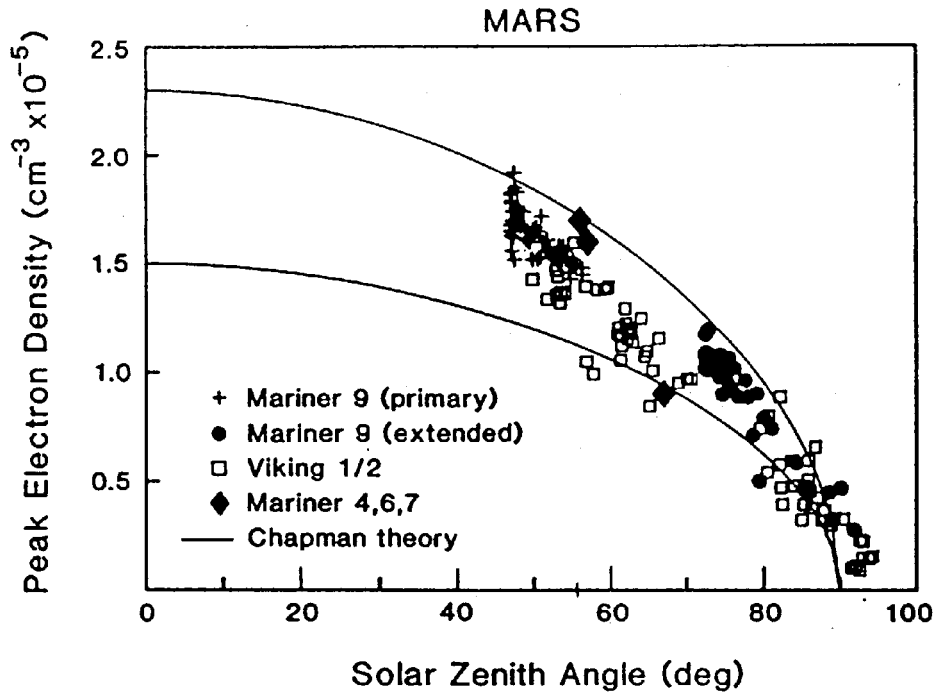


Figure 5

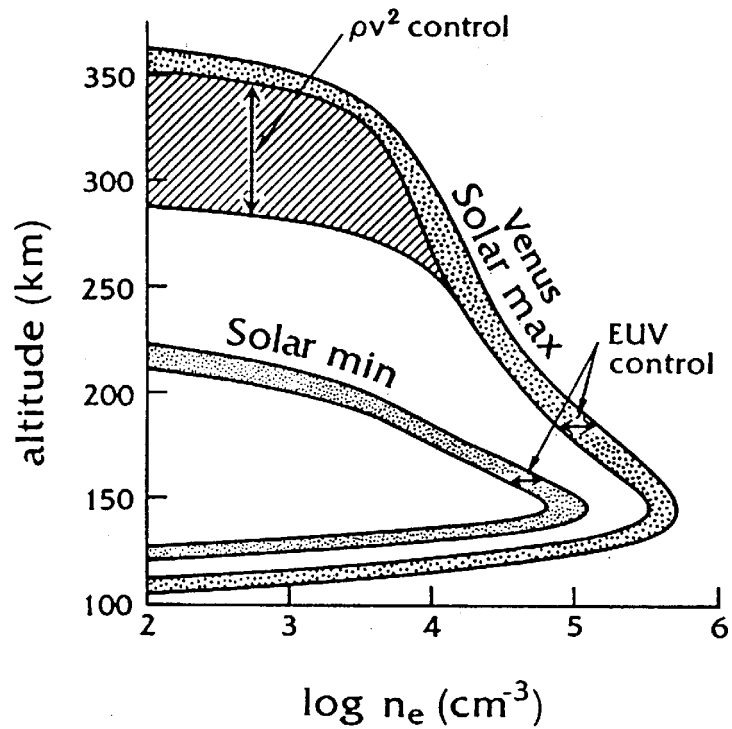


Figure 6